Received: 16 December 2016 | Revised: 19 September 2017 | Accepted: 22 September 2017

DOI: 10.1002/acs.2832

RESEARCH ARTICLE

WILEY

Coordinated semi-adaptive closed-loop control for infusion of two interacting medications

Xin Jin[1] | Chang-Sei Kim[1] | Steven T. Shipley[2] | Guy A. Dumont[3] | Jin-Oh Hahn[1]

[1]Department of Mechanical Engineering, University of Maryland, College Park, MD, USA

[2]Department of Pathology and Laboratory Medicine, University of North Carolina, Chapel Hill, NC, USA

[3]Department of Electrical and Computer Engineering, The University of British Columbia, Vancouver, BC, Canada

Correspondence
Jin-Oh Hahn, Department of Mechanical Engineering, University of Maryland, College Park, MD 20742, USA.
Email: jhahn12@umd.edu

Funding information
Office of Naval Research, Grant/Award Number: N000141410591 and N000141512018

Summary

This paper presents a coordinated and semi-adaptive closed-loop control approach to the infusion of 2 interacting medications. The proposed approach consists of an upper-level coordination controller and a lower-level semi-adaptive controller. The coordination controller recursively adjusts the reference targets based on the estimated dose-response relationship of a patient to ensure that they can be achieved by the patient. The semi-adaptive controller drives the patient outputs to the reference targets while estimating the patient's dose-response relationship online. In this way, the controller is resilient to unachievable caregiver-specified reference targets and responsive to the medication needs of individual patients. To establish the proposed approach, we developed the following: (1) a linear two-input–two-output dose-response model; (2) a two-input–two-output semi-adaptive controller to regulate the patient outputs while adapting high-sensitivity parameters in the patient model; and (3) a coordination controller to adjust the reference targets that reconcile caregiver inputs and medication use. The proposed approach was applied to an example scenario in which cardiac output and respiratory rate are regulated via infusion of propofol and remifentanil in an in silico simulation setting. The results show that the coordinated semi-adaptive control could (1) track achievable reference targets with consistent transient and steady-state performance and (2) resiliently adjust the unachievable reference targets to achievable ones.

KEYWORDS

coordinated control, direct dynamic dose-response model, medication infusion, model predictive control, model reference adaptive control, semi-adaptive control

1 | INTRODUCTION

There is an increasing interest in computerized closed-loop control of medication infusion for critically ill patients by virtue of its potential for delivery and continuous monitoring of high-quality treatment[1-3] and alleviation of caregivers' workload.[4,5] Indeed, closed-loop control of anesthesia,[6-8] vasopressor infusion,[9] and fluid resuscitation[10-12] has been an active area of research for a few decades. However, there are still at least two opportunities to further innovate and improve

Chang-Sei Kim is now with School of Mechanical Engineering, Chonnam National University, Gwangju, Korea.

closed-loop control of medication infusion as follows: (1) control design approaches for simultaneous infusion of multiple (and often synergistically interacting) medications and (2) coordination of reference targets.

Generally, multiple medications must be infused during the care of critically ill patients to achieve a multitude of treatment goals. However, the majority of prior art has focused on the infusion of a single medication, eg, propofol,[13-15] remifentanil,[16,17] and fluid,[18,19] whereas there is only limited volume of work reported on the closed-loop control for infusion of multiple medications to track multiple reference targets (see, for example, previous works[20-22]).

In addition to closed-loop control design, the coordination of reference targets also presents a challenge. In real clinical scenarios, reference targets are empirically specified by caregivers, eg, based on population norms and caregivers' experience. These ad hoc reference targets are not always achievable in all patients due to the interindividual variability in dose-response relationships and the bounds on medication dose to ensure patients' safety. In fact, inappropriate coordination of reference targets that cannot be achieved in a patient may potentially harm the patient via overdosing/underdosing. A critical challenge is that it is not possible to specify achievable reference targets for a patient before the treatment, since the dose-response relationship of the patient is typically not known a priori. Therefore, targets must be recursively adjusted by estimating the patient's dose-response relationship online while respecting the caregivers' therapeutic intent.

Existing well-known techniques for the adjustment of reference targets are reference governors and their variants, ie, add-on schemes used to avoid the violation of state and input constraints in a closed-loop control system by adjusting the reference targets during the transients.[23-25] However, these techniques are not appropriate to address the challenge at hand for at least two reasons. Most importantly, the primary goal of a reference governor is to keep the adjusted reference targets as close as possible to the original ones and ideally to ultimately bring them back to the original ones. In contrast, our goal is to adjust inherently unachievable reference targets to achievable ones so that the system (the patient in our case) can converge to the adjusted reference targets, while accounting for additional safety-critical considerations such as minimizing the total medication doses. Furthermore, a reference governor can only reduce the reference targets, whereas our goal is to adjust (ie, increase or decrease) reference targets according to the sensitivity of each patient to medications and their synergy. Therefore, novel approaches for coordinated adjustment of reference targets may be beneficial in providing closed-loop medication infusion control systems with resilience to inappropriate reference targets specified by caregivers, ultimately improving the safety of patients receiving medication treatments.

This paper presents a coordinated and semi-adaptive closed-loop control approach to the infusion of 2 interacting medications. The proposed approach consists of an upper-level coordination controller and a lower-level semi-adaptive controller. The coordination controller recursively adjusts the reference targets based on the estimated dose-response relationship of a patient to ensure that they can be achieved by the patient. The semi-adaptive controller drives the patient outputs to the reference targets while estimating the patient's dose-response relationship online. In this way, the controller is resilient to unachievable caregiver-specified reference targets and responsive to the medication needs of individual patients. To establish the proposed approach, we developed the following: (1) a linear two-input–two-output dose-response model; (2) a two-input–two-output semi-adaptive controller to regulate the patient outputs while adapting high-sensitivity parameters in the patient model; and (3) a coordination controller to adjust the reference targets that reconcile caregiver inputs and medication use. The proposed approach was applied to an example scenario in which cardiac output and respiratory rate are regulated via infusion of propofol and remifentanil in an in silico simulation setting.

This paper is organized as follows. Section 2 presents a control-oriented dose-response model for 2 interacting medications. Section 3 describes control architecture and design in detail. Section 4 presents and discusses in silico simulation testing. Section 5 concludes the paper with potential future directions.

2 | DOSE-RESPONSE MODEL FOR TWO INTERACTING MEDICATIONS

We developed a dose-response model for 2 interacting medications by combining a low-order mixing model reported in our previous works[16,26] and a response surface model reported in Minto et al[27] (see Figure 1). First, the low-order mixing model represents the relationship between the intravenous infusion rate and the (hypothetical) infusion rate at the site of action of a medication and is described as follows:

$$\begin{aligned}\dot{x}_1 &= -k_{e1}x_1 + k_{e1}u_1\\ \dot{x}_2 &= -k_{e2}x_2 + k_{e2}u_2,\end{aligned} \tag{1}$$

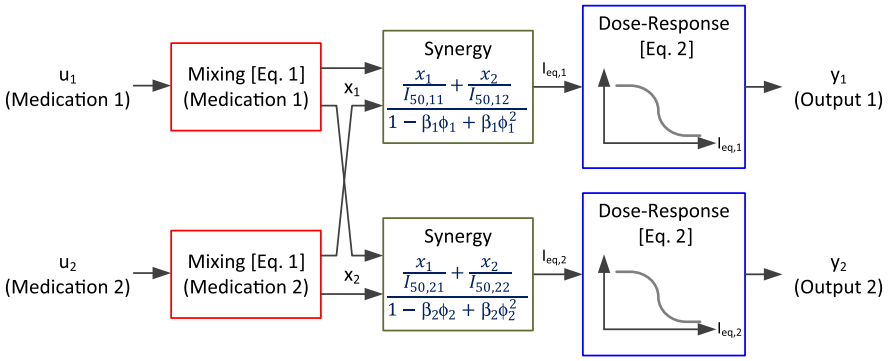

FIGURE 1 The dose-response model for 2 interacting medications consisting of a low-order mixing model and a response surface model [Colour figure can be viewed at wileyonlinelibrary.com]

where u_1 and u_2 are the intravenous infusion rates associated with the 2 medications M_1 and M_2, x_1 and x_2 are the corresponding infusion rates at the sites of action, and k_{e1} and k_{e2} are the equilibration constants. Second, the response surface model relates the 2 infusion rates to the system outputs (ie, clinical endpoints) and is described as follows:

$$\begin{aligned} y_1 &= y_{10}\left[1-\frac{\left(\frac{\frac{x_1}{I_{50,11}}+\frac{x_2}{I_{50,12}}}{1-\beta_1\phi_1+\beta_1\phi_1^2}\right)^{\gamma_1}}{1+\left(\frac{\frac{x_1}{I_{50,11}}+\frac{x_2}{I_{50,12}}}{1-\beta_1\phi_1+\beta_1\phi_1^2}\right)^{\gamma_1}}\right],\quad \phi_1=\frac{\frac{x_1}{I_{50,11}}}{\frac{x_1}{I_{50,11}}+\frac{x_2}{I_{50,12}}} \\ y_2 &= y_{20}\left[1-\frac{\left(\frac{\frac{x_1}{I_{50,21}}+\frac{x_2}{I_{50,22}}}{1-\beta_2\phi_2+\beta_2\phi_2^2}\right)^{\gamma_2}}{1+\left(\frac{\frac{x_1}{I_{50,21}}+\frac{x_2}{I_{50,22}}}{1-\beta_2\phi_2+\beta_2\phi_2^2}\right)^{\gamma_2}}\right],\quad \phi_2=\frac{\frac{x_1}{I_{50,21}}}{\frac{x_1}{I_{50,21}}+\frac{x_2}{I_{50,22}}}, \end{aligned} \tag{2}$$

where y_1 and y_2 are the system outputs, y_{10} and y_{20} are the baseline system outputs before the infusion starts, $I_{50,ij}$, $i,j=1,2$, is the infusion rate of medication M_j associated with 50% change in the system output i, and γ_1 and γ_2 are the cooperativity constants. The functions ϕ_1 and ϕ_2 denote the relative dominance of the infusion rates associated with the 2 medications ($\phi_1=\phi_2=1$ if only M_1 is infused and $\phi_1=\phi_2=0$ if only M_2 is infused). The parameters β_1 and β_2 represent the degree of synergistic interaction between the medications associated with the outputs y_1 and y_2 ($0<\beta_1,\beta_2<4$, where 0 and 4 correspond to zero and maximum interactions, respectively).

To derive a control-oriented input-output model relating y_1 and y_2 directly to u_1 and u_2, we transform Equation 2 as follows:

$$q_i \triangleq \left(\frac{y_{i0}-y_i}{y_i}\right)^{\frac{1}{\gamma_i}} = \frac{\frac{x_1}{I_{50,i1}}+\frac{x_2}{I_{50,i2}}}{1-\beta_i\phi_i(x_1,x_2)+\beta_i\phi_i^2(x_1,x_2)},\quad i=1,2, \tag{3}$$

which exhibits a large nonlinearity. To facilitate the control design, linearizing Equation 3 around an operating point (x_{10},x_{20}) yields the following:

$$\begin{aligned} q_i &\cong q_i(x_{10},x_{20})+\left.\frac{\partial q_i}{\partial x_1}\right|_{(x_{10},x_{20})}(x_1-x_{10})+\left.\frac{\partial q_i}{\partial x_2}\right|_{(x_{10},x_{20})}(x_2-x_{20}) \\ &= \frac{\left(\frac{x_{10}}{I_{50,i1}}+\frac{x_{20}}{I_{50,i2}}\right)^2\left[\left(\frac{x_{10}}{I_{50,i1}}\right)^2+(1+\beta_i)\left(\frac{x_{20}}{I_{50,i2}}\right)^2+2(1-\beta_i)\left(\frac{x_{10}}{I_{50,i1}}\right)\left(\frac{x_{20}}{I_{50,i2}}\right)\right]}{\left(\left(\frac{x_{10}}{I_{50,i1}}\right)^2+\left(\frac{x_{20}}{I_{50,i2}}\right)^2+(2-\beta_i)\left(\frac{x_{10}}{I_{50,i1}}\right)\left(\frac{x_{20}}{I_{50,i2}}\right)\right)^2}\frac{x_1}{I_{50,i1}} \\ &\quad+\frac{\left(\frac{x_{10}}{I_{50,i1}}+\frac{x_{20}}{I_{50,i2}}\right)^2\left[(1+\beta_i)\left(\frac{x_{10}}{I_{50,i1}}\right)^2+\left(\frac{x_{20}}{I_{50,i2}}\right)^2+2(1-\beta_i)\left(\frac{x_{10}}{I_{50,i1}}\right)\left(\frac{x_{20}}{I_{50,i2}}\right)\right]}{\left(\left(\frac{x_{10}}{I_{50,i1}}\right)^2+\left(\frac{x_{20}}{I_{50,i2}}\right)^2+(2-\beta_i)\left(\frac{x_{10}}{I_{50,i1}}\right)\left(\frac{x_{20}}{I_{50,i2}}\right)\right)^2}\frac{x_2}{I_{50,i2}}. \end{aligned} \tag{4}$$

Assuming M_1 and M_2 are primary and secondary medications, respectively, Equation 4 reduces to the following at $(x_{10}, x_{20}) = (x_{10}, 0)$:

$$\begin{aligned} q_1 &= \frac{x_1}{I_{50,11}} + (1+\beta_1)\frac{x_2}{I_{50,12}} = \frac{x_1}{I_{50,11}} + \rho_1\frac{x_2}{I_{50,12}} \triangleq \frac{x_1}{\lambda_{11}} + \frac{x_2}{\lambda_{12}} \\ q_2 &= \frac{x_1}{I_{50,21}} + (1+\beta_2)\frac{x_2}{I_{50,22}} = \frac{x_1}{I_{50,21}} + \rho_2\frac{x_2}{I_{50,22}} \triangleq \frac{x_1}{\lambda_{21}} + \frac{x_2}{\lambda_{22}}. \end{aligned} \tag{5}$$

Therefore, x_1 and x_2 can be expressed by q_1 and q_2 as follows:

$$\begin{aligned} x_1 &= \frac{\lambda_{11}\lambda_{21}}{\lambda_{12}\lambda_{21} - \lambda_{11}\lambda_{22}}(\lambda_{12}q_1 - \lambda_{22}q_2) \\ x_2 &= \frac{\lambda_{12}\lambda_{22}}{\lambda_{11}\lambda_{22} - \lambda_{12}\lambda_{21}}(\lambda_{11}q_1 - \lambda_{21}q_2). \end{aligned} \tag{6}$$

Now, differentiating Equation 5 in time yields the following:

$$\begin{aligned} \dot{q}_1 &= \frac{1}{\lambda_{11}}(-k_{e1}x_1 + k_{e1}u_1) + \frac{1}{\lambda_{12}}(-k_{e2}x_2 + k_{e2}u_2) \\ \dot{q}_2 &= \frac{1}{\lambda_{21}}(-k_{e1}x_1 + k_{e1}u_1) + \frac{1}{\lambda_{22}}(-k_{e2}x_2 + k_{e2}u_2). \end{aligned} \tag{7}$$

Finally, substituting Equation 6 into Equation 7 yields the following input-output model between q_1 and q_2 versus u_1 and u_2 for control design, where $\Delta \triangleq \lambda_{12}\lambda_{21} - \lambda_{11}\lambda_{22}$:

$$\begin{aligned} \dot{q}_1 &= \frac{1}{\Delta}(-k_{e1}\lambda_{12}\lambda_{21} + k_{e2}\lambda_{11}\lambda_{22})q_1 + \frac{k_{e1}}{\lambda_{11}}u_1 + \frac{1}{\Delta}(k_{e1}\lambda_{22}\lambda_{21} - k_{e2}\lambda_{21}\lambda_{22})q_2 + \frac{k_{e2}}{\lambda_{12}}u_2 \\ \dot{q}_2 &= \frac{1}{\Delta}(-k_{e1}\lambda_{12}\lambda_{11} + k_{e2}\lambda_{11}\lambda_{12})q_1 + \frac{k_{e1}}{\lambda_{21}}u_1 + \frac{1}{\Delta}(k_{e1}\lambda_{22}\lambda_{11} - k_{e2}\lambda_{21}\lambda_{12})q_2 + \frac{k_{e2}}{\lambda_{22}}u_2, \end{aligned} \tag{8}$$

which leads to the following linearly parameterized model:

$$\dot{\boldsymbol{q}} = \begin{bmatrix} \dot{q}_1 \\ \dot{q}_2 \end{bmatrix} = \boldsymbol{A}\begin{bmatrix} q_1 \\ q_2 \end{bmatrix} + \boldsymbol{B}\begin{bmatrix} u_1 \\ u_2 \end{bmatrix}, \tag{9}$$

where $\boldsymbol{A} = \frac{1}{\Delta}\begin{bmatrix} -k_{e1}\lambda_{12}\lambda_{21} + k_{e2}\lambda_{11}\lambda_{22} & k_{e1}\lambda_{22}\lambda_{21} - k_{e2}\lambda_{21}\lambda_{22} \\ -k_{e1}\lambda_{12}\lambda_{11} + k_{e2}\lambda_{11}\lambda_{12} & k_{e1}\lambda_{22}\lambda_{11} - k_{e2}\lambda_{21}\lambda_{12} \end{bmatrix}$ and $\boldsymbol{B} = \begin{bmatrix} \frac{k_{e1}}{\lambda_{11}} & \frac{k_{e2}}{\lambda_{12}} \\ \frac{k_{e1}}{\lambda_{21}} & \frac{k_{e2}}{\lambda_{22}} \end{bmatrix}$.

3 | CONTROL DESIGN AND EVALUATIONS

3.1 | Control architecture

The proposed control approach consists of an upper-level coordination controller and a lower-level semi-adaptive controller (see Figure 2). The coordination controller recursively adjusts the reference targets, based on the dose-response relationship of a patient estimated by the semi-adaptive controller and constraints imposed on the medication use, to ensure that the reference targets thus derived can be safely achieved by the patient. For given reference targets provided by the coordination controller, the semi-adaptive controller computes and executes the requisite medication infusion rates to guide the patient toward the reference targets while estimating the patient's dose-response relationship online and providing it to the coordination controller. Details on the design of coordination and semi-adaptive controllers are described in the following.

3.2 | Two-input–two-output semi-adaptive control

The model in Equation 9 is formulated in terms of the transformed (by Equation 3) outputs q_i rather than the actual ones y_i, $i = 1, 2$. To derive q_1 and q_2 from y_1 and y_2, γ_1 and γ_2 must be known. In a previous work, we have shown that γ_i makes relatively small influence on the system output compared with k_{ei} and $I_{50,ij}$ $(i, j = 1, 2)$ and may thus be fixed at a nominal value.[16] With γ_1 and γ_2 specified a priori, the model (9) is a linearly parameterized control design model with the elements of matrices $\boldsymbol{A}$ and $\boldsymbol{B}$ as unknowns to be adapted online. As the proposed control approach adapts only a subset of the plant model parameters (ie, parameters other than γ_1 and γ_2), it is semi-adaptive rather than fully adaptive.

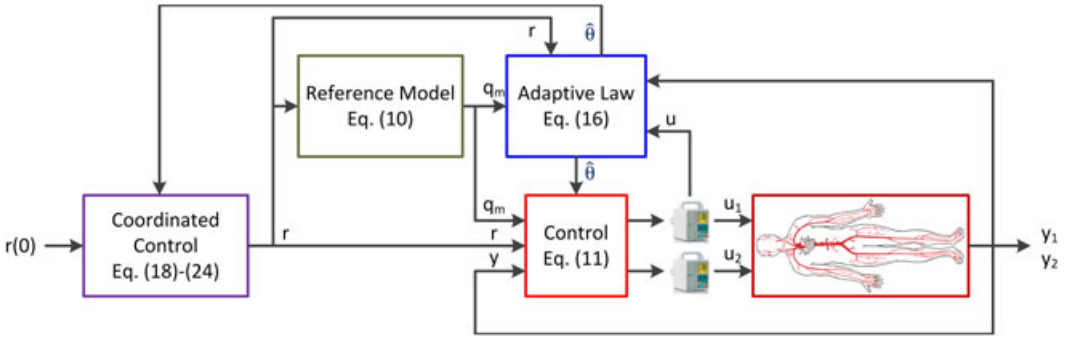

FIGURE 2 The architecture of coordinated semi-adaptive control [Colour figure can be viewed at wileyonlinelibrary.com]

Consider the following first-order reference model specifying the ideal endpoint responses of the patient to a reference target:

$$\dot{\boldsymbol{q}}_{\boldsymbol{m}} = \boldsymbol{A}_{\boldsymbol{m}}\boldsymbol{q}_{\boldsymbol{m}} + \boldsymbol{B}_{\boldsymbol{m}}\boldsymbol{r}, \tag{10}$$

where $\boldsymbol{A}_{\boldsymbol{m}} = -\begin{bmatrix} a_m & 0 \\ 0 & a_m \end{bmatrix} < \boldsymbol{0}$ is a negative definite matrix, $\boldsymbol{B}_{\boldsymbol{m}} = -\boldsymbol{A}_{\boldsymbol{m}}$, and $\boldsymbol{r}$ is a bounded reference target, ie, $\boldsymbol{r} = \begin{bmatrix} r_1 \\ r_2 \end{bmatrix}$. Then, the objective is to formulate an adaptive control law that can guide $\boldsymbol{y}$ to $\boldsymbol{y}_{\boldsymbol{m}}$ asymptotically, ie, $\lim_{t\to\infty}\boldsymbol{q}(t) - \boldsymbol{q}_{\boldsymbol{m}}(t) = 0$. Consider the following model reference adaptive control (MRAC) law:

$$\boldsymbol{u} = \begin{bmatrix} u_1 \\ u_2 \end{bmatrix} = \widehat{\boldsymbol{a}_{\boldsymbol{q}}}\begin{bmatrix} q_1 \\ q_2 \end{bmatrix} + \widehat{\boldsymbol{a}_{\boldsymbol{r}}}\begin{bmatrix} r_1 \\ r_2 \end{bmatrix} + \boldsymbol{\eta}\begin{bmatrix} q_1 - q_{1m} \\ q_2 - q_{2m} \end{bmatrix} = \widehat{\boldsymbol{a}_{\boldsymbol{q}}}\boldsymbol{q} + \widehat{\boldsymbol{a}_{\boldsymbol{r}}}\boldsymbol{r} + \boldsymbol{\eta}\boldsymbol{e}, \tag{11}$$

where $\widehat{\boldsymbol{a}_{\boldsymbol{q}}}$ and $\widehat{\boldsymbol{a}_{\boldsymbol{r}}}$ are variable feedback gains, $\boldsymbol{\eta} = -\begin{bmatrix} \eta_1 & 0 \\ 0 & \eta_2 \end{bmatrix} < \boldsymbol{0}$ is a negative definite constant feedback gain, r_1 and r_2 are the reference targets associated with the system outputs, and $\boldsymbol{e}$ is the tracking error. Note that the MRAC law (11) equipped with $\widehat{\boldsymbol{a}_{\boldsymbol{r}}} = \boldsymbol{a}_{\boldsymbol{r}} = \boldsymbol{B}^{-1}\boldsymbol{B}_{\boldsymbol{m}}$ and $\widehat{\boldsymbol{a}_{\boldsymbol{q}}} = \boldsymbol{a}_{\boldsymbol{q}} = \boldsymbol{B}^{-1}(\boldsymbol{A}_{\boldsymbol{m}} - \boldsymbol{A})$ results in perfect matching of the plant dynamics (9) to the reference model (10). Then, we have

$$\dot{\boldsymbol{q}} = \boldsymbol{A}\boldsymbol{q} + \boldsymbol{B}\boldsymbol{u} = \boldsymbol{A}\boldsymbol{q} + \boldsymbol{B}\left[\boldsymbol{B}^{-1}(\boldsymbol{A}_{\boldsymbol{m}} - \boldsymbol{A})\boldsymbol{q} + \boldsymbol{B}^{-1}\boldsymbol{B}_{\boldsymbol{m}}\boldsymbol{r} + \boldsymbol{\eta}\boldsymbol{e}\right] = \boldsymbol{A}_{\boldsymbol{m}}\boldsymbol{q} + \boldsymbol{B}_{\boldsymbol{m}}\boldsymbol{r} + \boldsymbol{B}\boldsymbol{\eta}\boldsymbol{e}. \tag{12}$$

However, the plant model parameters $\boldsymbol{a}_{\boldsymbol{r}}$ and $\boldsymbol{a}_{\boldsymbol{q}}$ are not known a priori in reality. Defining $\boldsymbol{\theta} \triangleq [\boldsymbol{a}_{\boldsymbol{q}} \quad \boldsymbol{a}_{\boldsymbol{r}}]$ and $\widehat{\boldsymbol{\theta}} \triangleq \left[\widehat{\boldsymbol{a}_{\boldsymbol{q}}} \quad \widehat{\boldsymbol{a}_{\boldsymbol{r}}}\right]$, the difference between the true versus estimated parameters is defined as follows:

$$\widetilde{\boldsymbol{\theta}} = \widehat{\boldsymbol{\theta}} - \boldsymbol{\theta} = \left[\widetilde{\boldsymbol{a}_{\boldsymbol{q}}} \quad \widetilde{\boldsymbol{a}_{\boldsymbol{r}}}\right] \triangleq \left[\widehat{\boldsymbol{a}_{\boldsymbol{q}}} - \boldsymbol{a}_{\boldsymbol{q}} \quad \widehat{\boldsymbol{a}_{\boldsymbol{r}}} - \boldsymbol{a}_{\boldsymbol{r}}\right]. \tag{13}$$

Then, the dynamics of the tracking error when the plant (9) is subject to the MRAC law (11) becomes the following:

$$\begin{aligned} \dot{\boldsymbol{e}} &= \dot{\boldsymbol{q}} - \dot{\boldsymbol{q}}_{\boldsymbol{m}} = \left(\boldsymbol{A} + \boldsymbol{B}\widehat{\boldsymbol{a}_{\boldsymbol{q}}}\right)\boldsymbol{q} + \boldsymbol{B}\widehat{\boldsymbol{a}_{\boldsymbol{r}}}\boldsymbol{r} + \boldsymbol{B}\boldsymbol{\eta}\boldsymbol{e} - \boldsymbol{A}_{\boldsymbol{m}}\boldsymbol{q}_{\boldsymbol{m}} - \boldsymbol{B}_{\boldsymbol{m}}\boldsymbol{r} \\ &= \left(\boldsymbol{A} + \boldsymbol{B}\widehat{\boldsymbol{a}_{\boldsymbol{q}}} - \boldsymbol{A}_{\boldsymbol{m}}\right)\boldsymbol{q} + \left(\boldsymbol{B}\widehat{\boldsymbol{a}_{\boldsymbol{r}}} - \boldsymbol{B}_{\boldsymbol{m}}\right)\boldsymbol{r} + \boldsymbol{A}_{\boldsymbol{m}}\boldsymbol{e} + \boldsymbol{B}\boldsymbol{\eta}\boldsymbol{e} \\ &= \boldsymbol{B}\widetilde{\boldsymbol{a}_{\boldsymbol{q}}}\boldsymbol{q} + \boldsymbol{B}\widetilde{\boldsymbol{a}_{\boldsymbol{r}}}\boldsymbol{r} + \boldsymbol{A}_{\boldsymbol{m}}\boldsymbol{e} + \boldsymbol{B}\boldsymbol{\eta}\boldsymbol{e} \\ &= \boldsymbol{B}\left[\widetilde{\boldsymbol{a}_{\boldsymbol{q}}} \quad \widetilde{\boldsymbol{a}_{\boldsymbol{r}}}\right]\begin{bmatrix} \boldsymbol{q} \\ \boldsymbol{r} \end{bmatrix} + \boldsymbol{A}_{\boldsymbol{m}}\boldsymbol{e} + \boldsymbol{B}\boldsymbol{\eta}\boldsymbol{e} = \boldsymbol{B}\widetilde{\boldsymbol{\theta}}\boldsymbol{\psi} + \boldsymbol{A}_{\boldsymbol{m}}\boldsymbol{e} + \boldsymbol{B}\boldsymbol{\eta}\boldsymbol{e} \end{aligned} \tag{14}$$

where $\boldsymbol{\psi} = \begin{bmatrix} \boldsymbol{q} \\ \boldsymbol{r} \end{bmatrix}$.

Assuming that all the leading principal minors of $\boldsymbol{B}$ are positive, there exists a positive definite matrix $\boldsymbol{P} = \begin{bmatrix} p_1 & 0 \\ 0 & p_2 \end{bmatrix} > \boldsymbol{0}$ such that $\boldsymbol{P}\boldsymbol{B} = \begin{bmatrix} p_1\frac{k_{e1}}{\lambda_{11}} & p_1\frac{k_{e2}}{\lambda_{12}} \\ p_2\frac{k_{e1}}{\lambda_{21}} & p_2\frac{k_{e2}}{\lambda_{22}} \end{bmatrix} > \boldsymbol{0}$ holds. Noting that all the elements in $\boldsymbol{B}$ assume positive values due to the physical meaning of the parameters k_{ei} and λ_{ij}, $i,j = 1,2$, there exist p_1 and p_2 making $\boldsymbol{P}\boldsymbol{B}$ symmetric, ie, satisfying $p_1\frac{k_{e2}}{\lambda_{12}} = p_2\frac{k_{e1}}{\lambda_{21}}$.

Hence, there exists a matrix $\boldsymbol{S}$ that satisfies $\boldsymbol{PB}=\boldsymbol{S}^{\boldsymbol{T}}\boldsymbol{S}$. Finally, consider the Lyapunov function $V=\boldsymbol{e}^{\boldsymbol{T}}\boldsymbol{Pe}+tr\left[\boldsymbol{S}\widetilde{\boldsymbol{\theta}}\boldsymbol{\Gamma}_{\boldsymbol{\theta}}^{-\mathbf{1}}\widetilde{\boldsymbol{\theta}}^{\boldsymbol{T}}\boldsymbol{S}^{\boldsymbol{T}}\right]$ and the adaptation law $\dot{\hat{\boldsymbol{\theta}}}^{\boldsymbol{T}}=-\boldsymbol{\Gamma}_{\boldsymbol{\theta}}\boldsymbol{\psi}\boldsymbol{e}^{\boldsymbol{T}}$, where $tr[\cdot]$ is the trace of the argument and $\boldsymbol{\Gamma}_{\boldsymbol{\theta}}$ is a positive definite adaptation gain matrix. Then, the time derivative of the Lyapunov function candidate reduces to the following:

$$\begin{aligned}\dot{V}&=\dot{\boldsymbol{e}}^{\boldsymbol{T}}\boldsymbol{Pe}+\boldsymbol{e}^{\boldsymbol{T}}\boldsymbol{P}\dot{\boldsymbol{e}}+tr\left[\boldsymbol{S}\dot{\widetilde{\boldsymbol{\theta}}}\boldsymbol{\Gamma}_{\boldsymbol{\theta}}^{-\mathbf{1}}\widetilde{\boldsymbol{\theta}}^{\boldsymbol{T}}\boldsymbol{S}^{\boldsymbol{T}}+\boldsymbol{S}\widetilde{\boldsymbol{\theta}}\boldsymbol{\Gamma}_{\boldsymbol{\theta}}^{-\mathbf{1}}\dot{\widetilde{\boldsymbol{\theta}}}^{\boldsymbol{T}}\boldsymbol{S}^{\boldsymbol{T}}\right]\\&=2\boldsymbol{e}^{\boldsymbol{T}}\boldsymbol{P}\dot{\boldsymbol{e}}+2tr\left[\boldsymbol{S}\widetilde{\boldsymbol{\theta}}\boldsymbol{\Gamma}_{\boldsymbol{\theta}}^{-\mathbf{1}}\dot{\widetilde{\boldsymbol{\theta}}}^{\boldsymbol{T}}\boldsymbol{S}^{\boldsymbol{T}}\right]\\&=2\boldsymbol{e}^{\boldsymbol{T}}\boldsymbol{P}\left(\boldsymbol{B}\widetilde{\boldsymbol{\theta}}\boldsymbol{\psi}+\boldsymbol{A}_{\boldsymbol{m}}\boldsymbol{e}+\boldsymbol{B}\boldsymbol{\eta}\boldsymbol{e}\right)-2tr\left[\boldsymbol{S}\widetilde{\boldsymbol{\theta}}\boldsymbol{\psi}\boldsymbol{e}^{\boldsymbol{T}}\boldsymbol{S}^{\boldsymbol{T}}\right]\\&=2\boldsymbol{e}^{\boldsymbol{T}}\boldsymbol{PB}\widetilde{\boldsymbol{\theta}}\boldsymbol{\psi}+2\boldsymbol{e}^{\boldsymbol{T}}\boldsymbol{PA}_{\boldsymbol{m}}\boldsymbol{e}+2\boldsymbol{e}^{\boldsymbol{T}}\boldsymbol{PB}\boldsymbol{\eta}\boldsymbol{e}-2\boldsymbol{e}^{\boldsymbol{T}}\boldsymbol{S}^{\boldsymbol{T}}\boldsymbol{S}\widetilde{\boldsymbol{\theta}}\boldsymbol{\psi}=2\boldsymbol{e}^{\boldsymbol{T}}\boldsymbol{PA}_{\boldsymbol{m}}\boldsymbol{e}+2\boldsymbol{e}^{\boldsymbol{T}}\boldsymbol{PB}\boldsymbol{\eta}\boldsymbol{e}\le 0.\end{aligned}\tag{15}$$

Since V is positive definite and $\dot{V}$ is negative semidefinite, V is bounded. Hence, the plant model (9) with the MRAC law (11) and the adaptation law $\dot{\hat{\boldsymbol{\theta}}}^{\boldsymbol{T}}=-\boldsymbol{\Gamma}_{\boldsymbol{\theta}}^{-\mathbf{1}}\boldsymbol{\psi}\boldsymbol{e}^{\boldsymbol{T}}$ is globally stable, and accordingly, $\boldsymbol{e}$, $\widetilde{\boldsymbol{a}_{\boldsymbol{q}}}$ and $\widetilde{\boldsymbol{a}_{\boldsymbol{r}}}$ are bounded. Then, $\dot{\boldsymbol{e}}$ is bounded from (14), and $\ddot{V}$ is also bounded from (15). As a consequence, $\dot{V}$ is uniformly continuous. Therefore, $\lim_{t\to\infty}\dot{V}=0$, and $\lim_{t\to\infty}\boldsymbol{e}(t)=\boldsymbol{0}$.

To prevent the drift in $\widehat{\boldsymbol{a}_{\boldsymbol{q}}}$ and $\widehat{\boldsymbol{a}_{\boldsymbol{r}}}$ while $\boldsymbol{e}(t)\cong\boldsymbol{0}$ (which frequently occurs in case the system is regulated at constant set points), we employed the dead zone,[28] a scheme to stop parameter adaptation when $\boldsymbol{e}(t)\cong\boldsymbol{0}$. We have

$$\dot{\hat{\boldsymbol{\theta}}}^{\boldsymbol{T}}=\begin{cases}-\boldsymbol{\Gamma}_{\boldsymbol{\theta}}\boldsymbol{\psi}\boldsymbol{e}^{\boldsymbol{T}}, & |e_1(t)|>\epsilon_{e_1}\ \text{or}\ \ |e_2(t)|>\epsilon_{e_2}\\ \boldsymbol{0}, & \text{otherwise.}\end{cases}\tag{16}$$

3.3 | Coordinated control via recursive reference adjustment

The primary role of the coordinated control is to keep the reference targets achievable by the system driven by the semi-adaptive control outlined in the previous section. In this paper, we developed a coordinated control scheme based on a recursive adjustment law for the reference targets by considering constraints on the following: (1) the input magnitudes (ie, bounds on the medication infusion rates) and energy (ie, total medication use) and (2) the degree of discrepancy between the original (ie, specified by the caregiver) versus adjusted reference targets. Details are as follows.

The set of achievable reference targets can be determined by the bounds imposed on the input and by the discrepancy between the originally specified versus adjusted reference targets as follows. First, in case of medication infusion, the elements of the input $\boldsymbol{u}$ must be positive while limited by an upper bound to ensure patient safety, ie, $0\le u_i\le\breve{u}_i$, $i=1,2$. Hence, considering (9), the reference targets must satisfy the following inequalities in the steady state:

$$0\le\boldsymbol{u}=\begin{bmatrix}u_1\\u_2\end{bmatrix}=\boldsymbol{B}^{-\mathbf{1}}\boldsymbol{A}\begin{bmatrix}r_1\\r_2\end{bmatrix}\le\begin{bmatrix}\breve{u}_1\\\breve{u}_2\end{bmatrix}.\tag{17}$$

Referring to (8), (17) yields the following pair of inequalities in terms of r_1 and r_2:

$$\begin{aligned}0\le\frac{\lambda_{11}\lambda_{12}\lambda_{21}}{\Delta}r_1-\frac{\lambda_{11}\lambda_{21}\lambda_{22}}{\Delta}r_2\le\breve{u}_1\ &\rightarrow\ \frac{\lambda_{22}}{\lambda_{12}}r_2\le r_1\le\frac{\lambda_{22}}{\lambda_{12}}r_2+\frac{\Delta\breve{u}_1}{\lambda_{12}\lambda_{11}\lambda_{21}}\\0\le\frac{\lambda_{12}\lambda_{21}\lambda_{22}}{\Delta}r_2-\frac{\lambda_{11}\lambda_{12}\lambda_{22}}{\Delta}r_1\le\breve{u}_2\ &\rightarrow\ \frac{\lambda_{21}}{\lambda_{11}}r_2-\frac{\Delta\breve{u}_2}{\lambda_{11}\lambda_{12}\lambda_{22}}\le r_1\le\frac{\lambda_{21}}{\lambda_{11}}r_2\end{aligned}\tag{18}$$

which altogether yields a parallelogram in the (r_1,r_2) space, as shown in Figure 3 (note that the parallelogram is guaranteed to exist because the slopes of the constraints in (18) satisfy $\frac{\lambda_{21}}{\lambda_{11}}>\frac{\lambda_{22}}{\lambda_{12}}$ given that all the leading principal minors of $\boldsymbol{B}$ are positive). Second, the discrepancy between the original (ie, caregiver specified) versus adjusted reference targets may be limited to respect the expertise of the caregiver, which results in the following inequalities in terms of r_1 and r_2 (note that these limits may be specified by the caregiver in advance):

$$r_{i0}-\epsilon_{r_i}\le r_i\le r_{i0}+\epsilon_{r_i},\quad i=1,2,\tag{19}$$

where r_{i0} is the originally specified value for r_i, $i=1,2$. These constraints altogether yield a rectangle in the (r_1,r_2) space, as shown in Figure 3. Finally, the set of achievable reference targets is determined as the intersection between the parallelogram and the rectangle, as shown in Figure 3.

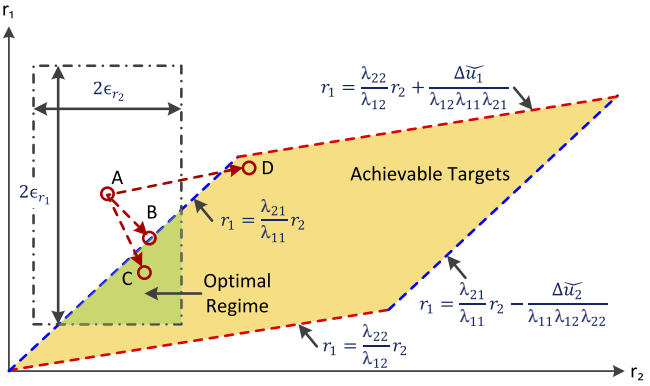

FIGURE 3 The set of achievable reference targets specified by the constraints on the input magnitudes and deviation from the original reference targets [Colour figure can be viewed at wileyonlinelibrary.com]

If the current pair of reference targets (r_1, r_2) is not achievable, one (and perhaps the easiest) way to make it achievable is to adjust it toward the nearest achievable pair of reference targets. From Figure 3, the nearest achievable pair can be found as the intersection between the side of the parallelogram having the smallest distance from the current pair of reference targets and the line perpendicular to the side that passes through the current pair of reference targets (eg, the pair "A" is adjusted toward "B"). However, this approach is not ideal in terms of input energy (ie, medication use) because the adjusted reference targets will be on a side of the parallelogram, at which $u_i = 0$ or $u_i = \breve{u}_i, i = 1, 2$, and the synergistic interaction between the 2 medications is not exploited to minimize the medication use. Hence, it may be sensible to penalize the medication use in determining the direction of adjustment of the reference targets to minimize the medication use. The optimal direction of adjustment, obtained by considering both the smallest distance to the set of achievable reference targets and input energy, may not be strictly perpendicular to the side of the parallelogram. Regardless, considering that all the sides of the parallelogram have positive slopes, adjusting r_1 and r_2 in the opposite direction (ie, if one is increased, the other must be decreased) is a viable requirement in adjusting the reference targets to effectively reach the achievable reference targets (eg, adjusting the pair "A" toward "C" is more effective than adjusting toward "D"). Hence, this can be enforced in the course of reference targets adjustment.

Summarizing the above considerations, we developed a coordinated control scheme based on a recursive adjustment law for the reference targets using the model predictive control formalism as follows. Consider a simple recursive adjustment law for r_1 and r_2 given by the following:

$$\dot{\boldsymbol{r}}(t) = \begin{bmatrix} \dot{r}_1(t) \\ \dot{r}_2(t) \end{bmatrix} = \boldsymbol{\Gamma_r} \begin{bmatrix} v_1(t) \\ v_2(t) \end{bmatrix} = \boldsymbol{\Gamma_r} \boldsymbol{v}(t), \tag{20}$$

where $\boldsymbol{\Gamma_r} = \begin{bmatrix} \gamma_{r_1} & 0 \\ 0 & \gamma_{r_2} \end{bmatrix}$ is a positive definite adaptation gain matrix and $\boldsymbol{v}(t)$ is the adjustment policy that is to be designed. Then, the dynamics of the plant (9), reference model (10), MRAC law (11), and reference target adjustment law (20) combined all together is given in the discrete-time domain by

$$\begin{aligned} \boldsymbol{q}(n+1) &= \boldsymbol{q}(n) + T_s \left\{ \left(\widehat{\boldsymbol{A}}(n) + \widehat{\boldsymbol{B}}(n)\widehat{\boldsymbol{a_q}}(n) + \widehat{\boldsymbol{B}}(n)\boldsymbol{\eta} \right) \boldsymbol{q}(n) - \widehat{\boldsymbol{B}}(n)\boldsymbol{\eta}\boldsymbol{q_m}(n) + \widehat{\boldsymbol{B}}(n)\widehat{\boldsymbol{a_r}}(n)\boldsymbol{r}(n) \right\} \\ \widehat{\boldsymbol{\theta}}^T(n+1) &= \begin{bmatrix} \widehat{\boldsymbol{a_q}}^T \\ \widehat{\boldsymbol{a_r}}^T \end{bmatrix} = \widehat{\boldsymbol{\theta}}^T(n) - T_s \left\{ \boldsymbol{\Gamma_\theta} \begin{bmatrix} \boldsymbol{q}(n) \\ \boldsymbol{r}(n) \end{bmatrix} \left[\boldsymbol{q}(n) - \boldsymbol{q_m}(n) \right]^T \right\} \\ \boldsymbol{q_m}(n+1) &= \boldsymbol{q_m}(n) + T_s \left\{ \boldsymbol{A_m}\boldsymbol{q_m}(n) + \boldsymbol{B_m}\boldsymbol{r}(n) \right\} \\ \boldsymbol{r}(n+1) &= \boldsymbol{r}(n) + T_s \boldsymbol{\Gamma_r} \boldsymbol{v}(n), \end{aligned} \tag{21}$$

with $\widehat{\boldsymbol{B}}(n) = \boldsymbol{B_m}\widehat{\boldsymbol{a_r}}^{-1}$ and $\widehat{\boldsymbol{A}}(n) = \boldsymbol{A_m} - \boldsymbol{B_m}\widehat{\boldsymbol{a_r}}^{-1}\widehat{\boldsymbol{a_q}}$. To reconcile constraints on the input magnitudes (18) and energy (ie, total medication use) and the degree of discrepancy between the original versus adjusted reference target (19), $\boldsymbol{v}(n)$, $t \le n \le t + N_c$ is determined by minimizing the following cost function, where N_c and N_p denote the control and prediction horizons, respectively:

$$J(n) = \sum_{n=t}^{t+N_p} \left[\rho_1 (r_1(n) - r_{10}(n))^2 + \rho_2 (r_2(n) - r_{20}(n))^2 + \rho_3 u_1^2(n) + \rho_4 u_2^2(n) \right] \tag{22}$$

subject to the linear inequality constraints (18) and (19), and the following nonlinear inequality constraints to ensure that r_1 and r_2 are adjusted in the opposite direction:

$$\delta_{\min} \leq \frac{v_2(n)}{v_1(n)} \leq \delta_{\max} \quad \rightarrow \quad \begin{cases} v_1(n)\left[v_2(n) - \delta_{\min} v_1(n)\right] \geq 0 \\ v_1(n)\left[v_2(n) - \delta_{\max} v_1(n)\right] \leq 0 \end{cases}, \quad t \leq n \leq t + N_c, \tag{23}$$

where $\delta_{\min} < \delta_{\max} < 0$.

At each sampling time step, the coordinated control problem is solved to yield $\boldsymbol{v}(n)$, $t \leq n \leq t + N_c$ that minimizes (22) subject to the dynamics (21) with the dose-response model parameters $\widehat{\boldsymbol{a}_q}$ and $\widehat{\boldsymbol{a}_r}$ adapted in the previous sampling time step as well as the constraints (18), (19), and (23). Then, $\boldsymbol{v}(t)$ is applied to the system to adjust the reference targets, which are tracked by the semi-adaptive controller while the patient's dose-response model parameters are adapted. This process is repeated at each sampling time step to guide the patient outputs to the (recursively adjusted) reference targets.

To prevent the drift in r_1 and r_2, we employed a dead-zone scheme to the coordinated controller, so that the adjustment of the reference targets are made only when v_1 and v_2 are sufficiently large. We have

$$r_i(n+1) = \begin{cases} r_i(n) + T_s \gamma_{r_i} v_i(n), & |v_1(n)| > \epsilon_{v_1} \text{ or } |v_2(n)| > \epsilon_{v_2} \\ r_i(n), & \text{otherwise,} \end{cases} \tag{24}$$

which, together with the dead-zone scheme employed in the adaptation law (16), helps to avoid unnecessary drift in the reference targets.

3.4 | In silico evaluation

To evaluate the proposed coordinated semi-adaptive control approach, we considered an example scenario in which cardiac output (y_1; $r_1(0)$=2.0 Lpm) and respiratory rate (y_2; $r_2(0)$=15 bpm) are regulated via infusion of propofol (M_1) and remifentanil (M_2) in an in silico simulation setting. We used the nonlinear dose-response model in (1)-(3) to simulate the dose-response relationships of a patient (note that our control design was performed based on the linear model (9), and the controller is subject to the structural uncertainty due to the modeling error originating from linearization). We specifically simulated pediatric patients based on the available dose-response data, by first setting the ranges of the model parameters and then creating a cohort of random patients. Details are as follows.

For the parameters associated with the dose-response relationships for propofol, we derived the ranges of k_{e1}, $I_{50,11}$, and γ_1 by analyzing the experimental data we obtained from swine subjects with body weight ranging 25 to 30 kg. Then, we derived the ranges of the remaining parameters associated with propofol by assuming that these ranges translate to pediatric patients of comparable body weight and (2) $I_{50,11} \approx I_{50,21}$.[29] The selected ranges for the parameters were $0.02 \leq k_{e1} \leq 0.10$ minutes^{-1}, $1 \leq \gamma_1 \leq 5$, $0.2 \leq I_{50,11} \leq 0.6$ mg/kg/min, and $0.2 \leq I_{50,21} \leq 0.6$ mg/kg/min.

For the parameters associated with the dose-response relationships for remifentanil, we derived the ranges of k_{e2}, $I_{50,22}$, and γ_2 from our previous work,[16] while we assumed that the influence of remifentanil on cardiac output is relatively small (translating to a large $I_{50,12}$). The selected ranges for the parameters were $0.10 \leq k_{e2} \leq 0.50$ minutes^{-1}, $1 \leq \gamma_2 \leq 5$, $0.12 \leq I_{50,12} \leq 0.36$ mcg/kg/min, and $0.04 \leq I_{50,22} \leq 0.12$ mcg/kg/min.

For the parameters associated with the intermedication interaction (ie, β_1 and β_2), we simply selected a wide range to simulate diverse intermedication interaction, ie, $0.5 \leq \beta_1, \beta_2 \leq 2$.

Based on the ranges of the model parameters selected above and assuming that all the model parameters exhibit uniform distributions within the selected ranges, we created 40 in silico patients by selecting a random value for each parameter from the respective range. We created these patients so that 20 of them can achieve the reference targets specified for the in silico simulation (ie, satisfy (18) with $r_1(0)$=2.0 Lpm and $r_2(0)$=15 bpm), whereas the remaining 20 patients cannot achieve them.

The weights in the cost function (22) were selected based on the in silico simulation result in an average patient, so that (1) the cost associated with the discrepancy between the original versus adjusted reference targets is 1000 times larger than the cost associated with the total medication use; (2) the costs associated with the 2 reference targets are equal; and (3) the costs associated with the 2 medications are equal.

In summary, the parameters associated with the coordinated semi-adaptive control were as follows: $\boldsymbol{A_m} = \begin{bmatrix} -0.8 & 0 \\ 0 & -0.8 \end{bmatrix} = -\boldsymbol{B_m}$, $\boldsymbol{\eta} = \begin{bmatrix} -5 & 0 \\ 0 & -5 \end{bmatrix}$, $\boldsymbol{\Gamma_\theta} = \boldsymbol{I}_{4\times 4}$, $\epsilon_{e_1} = 0.01$, $\epsilon_{e_2} = 0.01$, $\boldsymbol{\Gamma_r} = \begin{bmatrix} 60 & 0 \\ 0 & 60 \end{bmatrix}$, $N_c = 2$, $N_p = 20$, $\rho_1 = 1000$, $\rho_2 = 825.5$, $\rho_3 = 1$, $\rho_4 = 40$, $\widetilde{u_1} = 0.8$ mg/kg/min, $\widetilde{u_2} = 0.07$ mcg/kg/min, $\epsilon_{r_1} = 0.3$, $\epsilon_{r_2} = 0.3$, $\delta_{\min} = -2$, $\delta_{\max} = -0.5$, $\epsilon_{v_1} = 0.02$, $\epsilon_{v_2} = 0.02$.

In the in silico evaluation, nominal cardiac output and respiratory rate before medication infusion were set at 3.0 Lpm and 25 bpm. The initial model parameter values in the controller were set at the respective average values from all the patients. For control computation, a sampling rate of 1 Hz was used. Considering that higher infusion rates (eg, bolus infusion) are required for reference target tracking during the initial transients, we allowed higher propofol (4 mg/kg/min) and remifentanil (0.36 mcg/kg/min) infusion rates during the first 10 minutes after the control action started.

We examined 3 key aspects related to the performance of the coordinated semi-adaptive control. First, we examined the performance of semi-adaptive control compared with nonadaptive control. For this purpose, we conducted in silico evaluation of semi-adaptive versus nonadaptive controllers using the 20 in silico patients with achievable reference target. Second, we examined the performance of coordinated semi-adaptive control compared with the same semi-adaptive control without reference target adjustment. For this purpose, we conducted in silico evaluation of coordinated versus noncoordinated semi-adaptive controllers using the 20 in silico patients with unachievable reference target. Third, we examined the detailed behavior of the coordinated controller, especially the way it reconciles the constraints on (1) the infusion rate limits and total medication use versus (2) the degree of discrepancy between the original versus adjusted reference targets, as the values of the weights in the cost function (22) vary.

4 | RESULTS AND DISCUSSION

4.1 | Semi-adaptive control

Figure 4 presents the in silico simulation testing results associated with the semi-adaptive and nonadaptive controllers in the 20 patients with achievable reference targets. The semi-adaptive controller was superior to its nonadaptive counterpart both during the transient ($0 \le t \le 5$ minutes) and steady state. On the average, the semi-adaptive controller could reduce the transient reference tracking errors associated with cardiac output and respiratory rate by 15% and 21%, respectively (in terms of root-mean-squared error), and the steady-state errors (in the absolute sense) by 5% and 83%, respectively. In addition, the variances associated with all these errors were consistently smaller in the semi-adaptive than nonadaptive controller. Considering that the main rationale underpinning the development of semi-adaptive control is to ensure robust performance against large interindividual variability in dose-response relationships, the efficacy of the semi-adaptive control can be deemed satisfactory if not excellent.

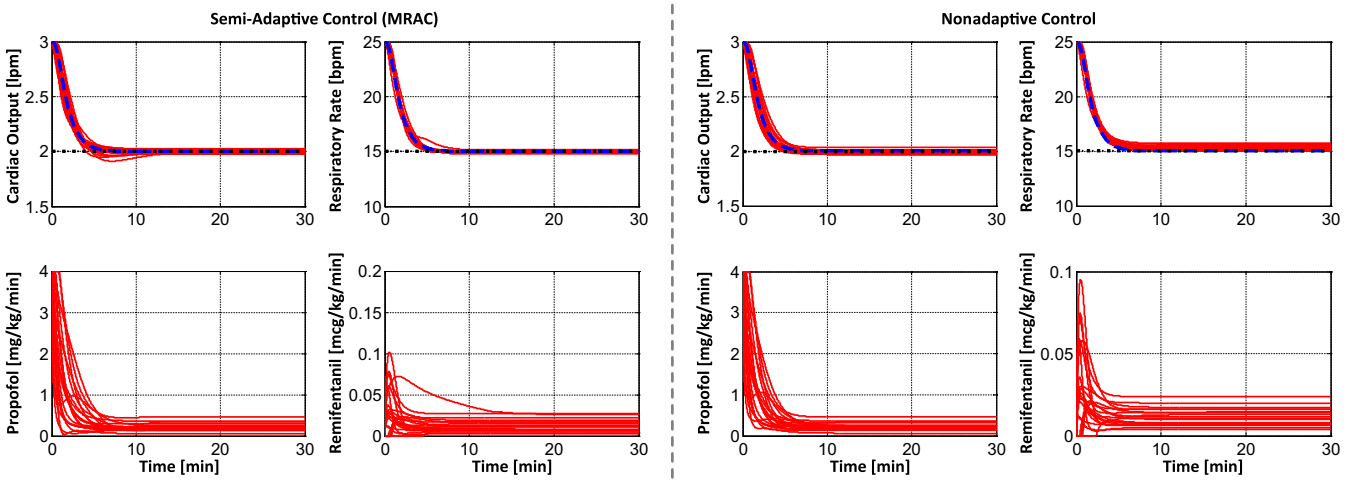

FIGURE 4 In silico simulation testing results associated with the semi-adaptive and nonadaptive controls in the 20 patients with achievable reference targets. MRAC, model reference adaptive control [Colour figure can be viewed at wileyonlinelibrary.com]

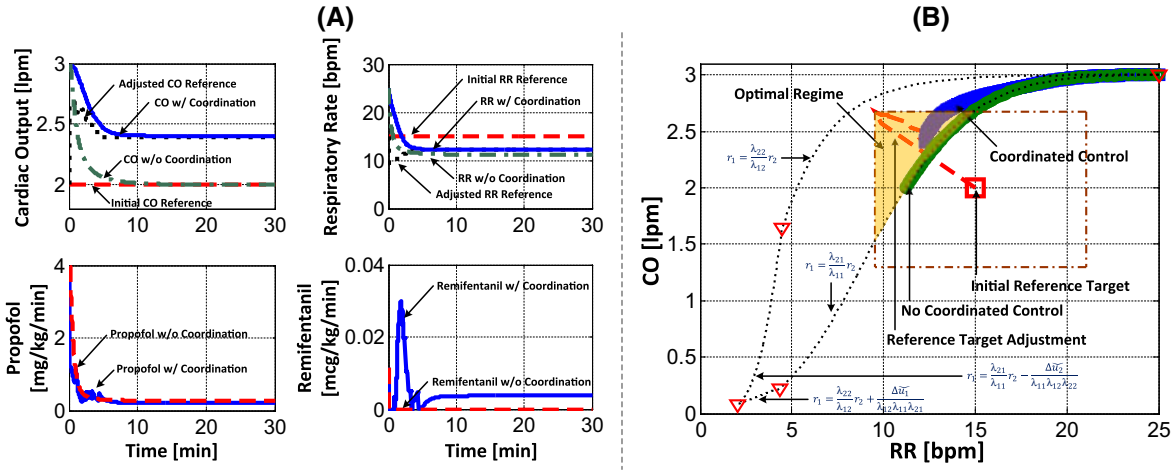

FIGURE 5 The evolution of adjusted reference targets and system outputs associated with the coordinated semi-adaptive control in a patient with unachievable reference targets. A, Time plots; B, Phase plot [Colour figure can be viewed at wileyonlinelibrary.com]

4.2 | Coordinated semi-adaptive control

Figure 5 presents a representative example of the evolution of adjusted reference targets and system outputs associated with the coordinated semi-adaptive control in a patient with unachievable reference targets. The result demonstrates that the initially specified unachievable reference targets are adjusted toward the optimal regime (shown in Figure 3) and the semi-adaptive control guides the patient to these new achievable reference targets as time evolves. In contrast, the system outputs converge to a point on the parallelogram in case the coordinated control is not employed, which means that at least one input is saturated with large steady-state error(s). This desired behavior was consistently observed in all patients.

Overall, the coordinated controller could largely reduce the overall reference tracking errors associated with cardiac output (60%) and respiratory rate (96%) over the entire in silico simulation ($0 \le t \le 30$ minutes) and the steady-state error associated with respiratory rate (99% in the absolute sense), compared with when the coordinated controller was not employed to adjust the reference targets (see Figure 6). In addition, the coordinated controller could also decrease propofol use while increasing remifentanil use, by adjusting the reference targets so that intermedication synergy can be exploited

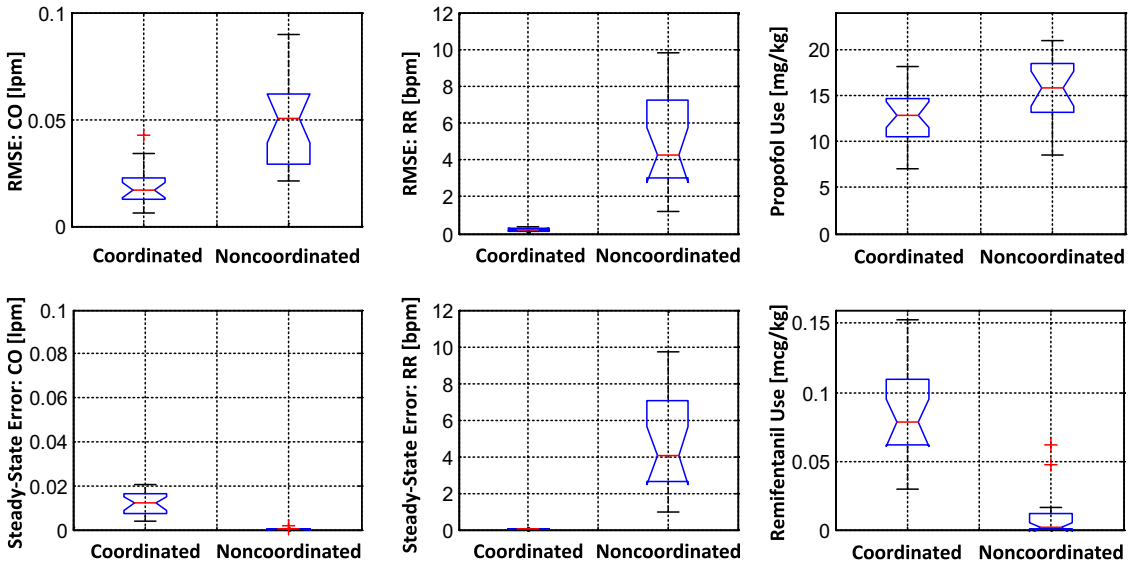

FIGURE 6 Distribution of the overall reference tracking and steady-state errors and the total medication use associated with semi-adaptive control in the presence/absence of coordinated control. RMSE, root-mean-squared error [Colour figure can be viewed at wileyonlinelibrary.com]

more effectively (see Figure 6). The steady-state error associated with cardiac output was relatively large with the coordinated controller. This was due to the dead zone implemented for the parameter adaptation law in (16). In the absence of coordinated controller, the adaptation law was persistently enabled to drive cardiac output error to zero because the tracking error associated with respiratory rate was large (since its reference target could not be reached) and the dead zone was never activated. On the other hand, the coordinated controller activated the dead zone by adjusting the reference targets, thereby allowing the tracking errors to become small. Noting that the dead zone for cardiac output in (16) was 0.03 Lpm and that the steady-state cardiac output error was consistently smaller than 0.03 Lpm, these errors were deemed acceptable.

It is worthwhile to scrutinize the behavior of the system inputs and outputs pertinent to the particular in silico simulation conducted in this paper to glean more insights on the coordinated controller. From our in silico simulation, a large decrease in the respiratory rate error and a large increase in the remifentanil use were consistently observed. However, the changes associated with the cardiac output error and propofol were relatively small. We speculate that these observations may be interpreted as follows. First, the dose-response model parameters we employed in the in silico simulation dictate that the cardiac output is primarily influenced by propofol, whereas the respiratory rate is influenced by both propofol and remifentanil. Second, the propofol infusion rate required to achieve the original cardiac output target ($r_1(0)$=2.0 Lpm) in the steady state leads to steady-state respiratory rate lower than the original respiratory rate target ($r_2(0)$=15 bpm) on the average. Hence, the coordinated controller increases the reference target for cardiac output (as realized by a decrease in r_1; see Figure 5) and decreases the reference target for respiratory rate (as realized by an increase in r_2; see Figure 5) to decrease the required propofol infusion rate and increase the required remifentanil infusion rate while exploiting the synergy between the two. In this way, the coordinated controller fulfills the desired objectives of driving unachievable reference targets to achievable ones and, at the same time, minimizing the total medication use. It is noted that the proposed control approach exhibited consistent performance regardless of the location of the original reference targets in our in silico simulation testing.

4.3 | Dependence of coordinated semi-adaptive control on cost function weights

On the average, the coordinated controller exhibited intuitively relevant behaviors as the weights in the cost function (22) were varied, as described in the following (see Figure 7).

First, when the penalty on the control energy terms is increased relative to the discrepancy between the original versus adjusted reference targets (by simultaneously altering ρ_3 and ρ_4; see Figure 7A), the coordinated controller decreases propofol and remifentanil uses. This leads to a decrease in r_1 and r_2 via an increase in the reference targets for cardiac output and respiratory rate (note that r_1 and r_2 are specified in terms of q_1 and q_2). Then, noting that $r_1 < r_1(0)$ and

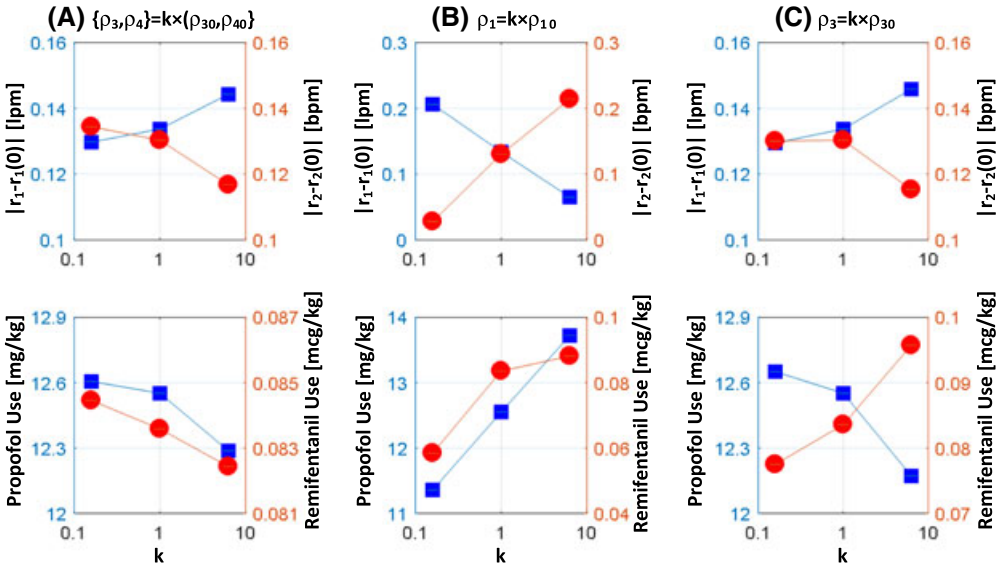

FIGURE 7 Dependence of the behavior of coordinated semi-adaptive control on cost function weights. The left and right axes apply to squares and circles, respectively [Colour figure can be viewed at wileyonlinelibrary.com]

$r_2 > r_2(0)$ under the nominal weights in our in silico simulation testing (see Figure 5A,B), $|r_1 - r_1(0)|$ increases while $|r_2 - r_2(0)|$ decreases.

Second, when the penalty on the discrepancy between the original versus adjusted cardiac output reference target is increased relative to other penalties (by altering ρ_1; see Figure 7B), the coordinated controller decreases $|r_1 - r_1(0)|$. To still drive the reference targets toward the optimal regime (see Figure 3) while limiting $|r_1 - r_1(0)|$, it increases $|r_2 - r_2(0)|$. Since $r_1 < r_1(0)$ and $r_2 > r_2(0)$ under the nominal weights in our in silico simulation testing, this leads to a decrease in cardiac output and respiratory rate reference targets and, accordingly, an increase in propofol and remifentanil uses. The opposite behavior is observed when ρ_2 is altered instead (not shown).

Third, when the penalty on the propofol use is increased relative to the other penalties (by altering ρ_3; see Figure 7C), the coordinated controller decreases propofol use while increases remifentanil use. This leads to a decrease in r_1, and since $r_1 < r_1(0)$, an increase in $|r_1 - r_1(0)|$. In addition, a decrease propofol use, which is relatively large compared with the increase in remifentanil use, results in the corresponding decrease in r_2 and (since $r_2 > r_2(0)$) $|r_2 - r_2(0)|$. The opposite behavior is observed when ρ_4 is altered instead, though the extent is relatively small (not shown).

The abovementioned intuitive behaviors of the proposed coordinated semi-adaptive control approach may be useful in tuning the weights in the cost function (22) to customize its performance when applied to other medication infusion problems.

5 | CONCLUSIONS

We have proposed and in silico validated a coordinated semi-adaptive closed-loop control approach to the infusion of 2 interacting medications. We demonstrated that the proposed approach could (1) achieve consistent reference target tracking in the presence of large interindividual variability in dose-response relationships and (2) adjust unachievable reference targets to achievable ones while minimizing the medication use by exploiting the intermedication synergy.

This study has ample rooms for future improvements and extensions. First, the proposed approach was validated only in an in silico scenario with an exemplary medication pair. To examine the generalizability of the approach, a follow-up work is required on rigorous in silico testing with diverse medication pairs. In addition, efforts toward preclinical and clinical trials must be made, especially in collaboration with the regulatory sector, before the approach, and closed-loop medication infusion in general, can be deployed with solid safety guarantee for widespread adoption. Second, the proposed approach, in its current development, is applicable only to control of 2 medications. To maximize its potential, a follow-up work is required on the extension of the approach to coordinated control of multiple (>2) medications.

ACKNOWLEDGEMENT

This material is based on the work supported by the Office of Naval Research under grants N000141410591 and N000141512018. Any opinions, findings, and conclusions or recommendations expressed in this material are those of the authors and do not necessarily reflect the views of the Office of Naval Research.

ORCID

Jin-Oh Hahn http://orcid.org/0000-0001-5429-2836

REFERENCES

1. Puri GD, Kumar B, Aveek J. Closed loop anaesthesia delivery system (CLADS) - anaesthesia robot. *Anaesth Intensive Care*. 2007;35(3):357.
2. Hemmerling TM, Charabati S, Zaouter C, Minardi C, Mathieu PA. A randomized controlled trial demonstrates that a novel closed-loop propofol system performs better hypnosis control than manual administration. *Can J Anesth*. 2010;57(8):725-735.
3. Sieber TJ, Frei CW, Derighetti M, Feigenwinter P, Leibundgut D, Zbinden AM. Model-based automatic feedback control versus human control of end-tidal isoflurane concentration using low-flow anaesthesia. *Br J Anaesth*. 2000;85(6):818-825.
4. Dussaussoy C, Peres M, Jaoul V, et al. Automated titration of propofol and remifentanil decreases the anesthesiologist's workload during vascular or thoracic surgery: a randomized prospective study. *J Clin Monit Comput*. 2014;28(1):35-40.
5. Dumont GA, Ansermino JM. Closed-loop control of anesthesia: a primer for anesthesiologists. *Anesth Analg*. 2013;117(5):1130-1138.
6. Ionescu CM, Keyser RD, Torrico BC, Smet TD, Struys MM, Normey-Rico JE. Robust predictive control strategy applied for propofol dosing using BIS as a controlled variable during anesthesia. *IEEE Trans Biomed Eng*. 2008;55(9):2161-2170.

7. Méndez JA, Torres S, Reboso JA, Reboso H. Adaptive computer control of anesthesia in humans. *Comput Methods Biomech Biomed Engin*. 2009;12(6):727-734.
8. Haddad WM, Hayakawa T, Bailey JM. Adaptive control for non-negative and compartmental dynamical systems with applications to general anesthesia. *Int J Adapt Control Signal Process*. 2003;17(3):209-235.
9. Sng BL, Tan HS, Sia ATH. Closed-loop double-vasopressor automated system vs manual bolus vasopressor to treat hypotension during spinal anaesthesia for caesarean section: a randomised controlled trial. *Anaesthesia*. 2014;69(1):37-45.
10. Salinas J, Drew G, Gallagher J, et al. Closed loop and decision assist resuscitation of burn patients. *J Trauma Acute Care Surg*. 2008;64(4):S321-S332.
11. Rinehart J, Lee C, Canales C, Kong A, Kain Z, Cannesson M. Closed-loop fluid administration compared to anesthesiologist management for hemodynamic optimization and resuscitation during surgery: an in vivo study. *Anesth Analg*. 2013;117(5):1119-1129.
12. Rinehart J, Chung E, Canales C, Cannesson M. Intraoperative stroke volume optimization using stroke volume, arterial pressure, and heart rate: closed-loop (learning intravenous resuscitator) versus anesthesiologists. *J Cardiothorac Vasc Anesth*. 2012;26(5):933-939.
13. van Heusden K, Dumont GA, Soltesz K, et al. Design and clinical evaluation of robust PID control of propofol anesthesia in children. *IEEE Trans Control Syst Technol*. 2014;22(2):491-501.
14. De Smet T, Struys MMRF, Neckebroek MM, den Hauwe KV, Bonte S, Mortier EP. The accuracy and clinical feasibility of a new Bayesian-based closed-loop control system for propofol administration using the bispectral index as a controlled variable. *Anesth Analg*. 2008;107(4):1200-1210.
15. Niño J, De Keyser R, Syafiie S, Ionescu C, Struys M. EPSAC-controlled anesthesia with online gain adaptation. *Int J Adapt Control Signal Process*. 2009;23(5):455-471.
16. Jin X, Kim C-S, Dumont GA, Ansermino JM, Hahn J-O. A semi-adaptive control approach to closed-loop medication infusion. *Int J Adapt Control Signal Process*. 2017;31(2):240-254.
17. Hemmerling TM, Charabati S, Salhab E. The Analgoscore TM: a novel score to monitor intraoperative nociception and its use for closed-loop application of remifentanil. *Anesthesiology*. 2009;4(4):311-318.
18. Kramer GC, Kinsky MP, Prough DS, et al. Closed-loop control of fluid therapy for treatment of hypovolemia. *J Trauma*. 2008;64(4):S333-S341.
19. Chaisson NF, Kirschner RA, Deyo DJ, Lopez JA, Prough DS, Kramer GC. Near-infrared spectroscopy-guided closed-loop resuscitation of hemorrhage. *J Trauma*. 2003;54(5):S183-S192.
20. Shieh JS, Abbod MF, Hsu CY, Huang SJ, Han YY, Fan SZ. Monitoring and control of anesthesia using multivariable self-organizing fuzzy logic structure. *Stud Fuzziness Soft Comput*. 2009;242:273-295.
21. Lu Q, Mahfouf M. Multivariable self-organizing fuzzy logic control using dynamic performance index and linguistic compensators. *Eng Appl Artif Intel*. 2012;25(8):1537-1547.
22. Simanski O, Janda M, Schubert A, Bajorat J, Hofmockel R, Lampe B. Progress of automatic drug delivery in anaesthesia—the Rostock assistant system for anaesthesia control (RAN). *Int J Adapt Control Signal Process.* 2009;23(5):504-521.
23. Kolmanovsky I, Garone E, Di Cairano S. Reference and command governors: A tutorial on their theory and automotive applications. Paper presented at: Proceedings of the American Control Conference; 2014; Portland, Oregon.
24. Gilbert E, Kolmanovsky I, Tan KT. Discrete-time reference governors and the nonlinear control of systems with state and control constraints. *Int J Robust Nonlinear Control*. 1995;5(5):487-504.
25. Gilbert EG, Ong CJ. Constrained linear systems with hard constraints and disturbances: an extended command governor with large domain of attraction. *Automatica*. 2011;47(2):334-340.
26. Hahn JO, Dumont GA, Ansermino JM. A direct dynamic dose-response model of propofol for individualized anesthesia care. *IEEE Trans Biomed Eng*. 2012;59(2):571-578.
27. Minto CF, Schnider TW, Short TG, Gregg KM, Gentilini A, Shafer SL. Response surface model for anesthetic drug interactions. *Anesthesiology*. 2000;92(6):1603-1616.
28. Slotine JJ, Li W. *Applied Nonlinear Control*. Englewood Cliffs, NJ: Prentice Hall; 1991.
29. Koroglu A, Teksan H, Sagir O, Yucel A, Toprak HI, Ersoy OM. A comparison of the sedative, hemodynamic, and respiratory effects of dexmedetomidine and propofol in children undergoing magnetic resonance imaging. *Anesth Analg*. 2006;103(1):63-67.

How to cite this article: Jin X, Kim C-S, Shipley ST, Dumont GA, Hahn J-O. Coordinated semi-adaptive closed-loop control for infusion of two interacting medications. *Int J Adapt Control Signal Process*. 2018;32:134–146. https://doi.org/10.1002/acs.2832